

Application of Dual-Function Microgels in Ultraviolet/Thermal Dual-Cure Clear Coats

Seung Man Noh,^{1,2} Jaekyu Min,³ Jae Woo Lee,¹ Hyun Wook Jung,² Jong Myung Park⁴

¹PPG Industries Korea, Cheonan 330-912, Korea

²Department of Chemical and Biological Engineering, Korea University, Seoul 136-713, Korea

³Pohang Institute of Metal Industry Advancement, Pohang 790-834, Korea

⁴Graduate Institute of Ferrous Technology, Pohang University of Science and Technology, Pohang 790-834, Korea

Received 27 September 2011; accepted 11 January 2012

DOI 10.1002/app.36796

Published online in Wiley Online Library (wileyonlinelibrary.com).

ABSTRACT: Hydroxyl-functional nanosized microgels were synthesized by nonaqueous dispersion polymerization with caprolactone-modified hydroxyethyl acrylate as a stabilizer and 1,6-hexanediol diacrylate as a crosslinker. The dual-function microgels were prepared by the reaction of the hydroxyl groups of the microgel with isocyanatoethyl methacrylate for use in a UV/thermal dual-cure process. The synthesized microgels were identified by Fourier transform infrared spectroscopy, transmission electron microscopy, and dynamic light scattering. The effects of the addition of the microgels on the rheological properties, curing behavior, and film properties were also investi-

gated. The addition of the microgels resulted in a lower viscosity and shear thinning behavior in the coating solution. The glass-transition temperature of the cured films decreased with the addition of the microgels because of the flexible functional stabilizer chain that could participate in UV and thermal crosslinking. The scratch resistance of the cured coating also increased because of the increased ductility of the film caused by the soft microgel. © 2012 Wiley Periodicals, Inc. *J. Appl. Polym. Sci.* 000: 000–000, 2012

Key words: coatings; microgels; nanotechnology

INTRODUCTION

UV curing technology has been widely used in the manufacturing of printing inks, protective coatings, varnishes, adhesives, and composite materials.^{1–3} The main advantages of UV curing are a high curing speed, reduced energy consumption, compatibility with heat-sensitive substrates, and low organic emissions. A UV-curable coating is usually applied on a flat substrate, such as metal, plastic, or wood, because a uniform UV illumination of the coating is required to obtain good coating properties. Currently, there is a growing demand for the application of UV-curable coatings to three-dimensional substrates. The practical aspects with regard to the design of UV beams used to obtain the uniform illumination of large irregular objects have been addressed; however, shadow areas that cannot be reached by UV radiation remain a problem. To solve this UV shadowing issue, dual-cure coating systems that combine UV and thermal treatments have been

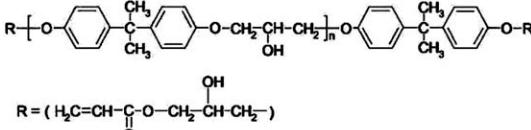
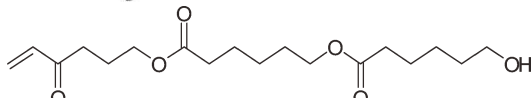
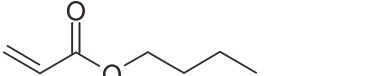
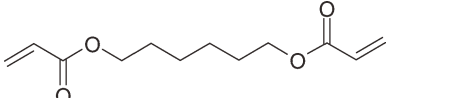
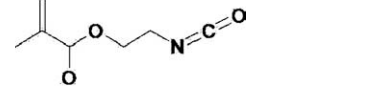
developed.^{4,5} The binder for UV/thermal dual-cure processes typically contains different types of functional groups that act simultaneously; for example, acrylate is functional in UV curing, and hydroxyl groups are functional in thermal curing.

A *polymeric microgel* is a crosslinked polymer particle with a network structure within a solvent. Microgels have been widely used as additives in high-performance organic coatings because of their rheological and reinforcing properties. In recent decades, there has been considerable interest in the preparation of polymeric microgels in which the size, surface features, and functionalities can be controlled.^{6–8} Functional groups in microgels can not only affect the rheological properties of the coating solution but can also influence the mechanical properties by crosslinking within the matrix. Epoxy/carboxylic acid functional microgels have been used in epoxy matrices to improve their toughness.⁹ (Meth)acrylate-functional microgels have been used as crosslinking agents, and their use has improved the mechanical properties of UV curing matrices.¹⁰ Water-based baking paints made from a reactive microgel and melamine–formaldehyde resin showed better coating properties and a better dispersability of aluminum powder compared to conventional paints.¹¹ Epoxy–acrylic microgels prepared via aqueous dispersion polymerization showed increased corrosion resistance at the edges of electrodeposited

Correspondence to: H. W. Jung (hwjung@grtrkr.korea.ac.kr) or J. M. Park (jongpark@postech.ac.kr).

Contract grant sponsor: Korean National Cleaner Production—Industrial Strategic Technology Development Program; contract grant number: 2008-E004-00.

TABLE I
Chemical Formulas of the Monomers Used in This Study

Name	Designation	Chemical structure
Epoxy-acrylate	EA	
Caprolactone-modified hydroxyethyl acrylate	CHA	
Butyl acrylate	BA	
1,6-Hexanediol diacrylate	HDDA	
2-Isocyanatoethyl methacrylate	IEM	

steel substrates when they were added to coating formulations.¹²

When microgels are used in a clear coat, the particle size of the microgel should be smaller than the shortest visible light wavelength to sustain the coating transparency. Nanosized crosslinked microgels can be prepared by dispersion polymerization with the combination of a stabilizer, a crosslinking agent, and monomers.¹³ The stabilizer carries out particle stabilization through steric hindrance. In addition, the fully stretched stabilizer chains can affect the compatibility between the microgel and other binders in the coating solution. The stabilizer, which has long linear hydrocarbon chains, can stabilize the microgel particles but can also cause compatibility problems when used with common coating binders, such as epoxy, acrylics, and polyester.

In this study, we synthesized nanosized polymeric microgels containing hydroxyl and methacrylate functional groups for dual-curable coatings by nonaqueous dispersion polymerization. The hydroxyl-functional microgel (HFM) was synthesized with caprolactone-modified hydroxyethyl acrylate (CHA), which has a terminal hydroxyl group as the stabilizer monomer. UV-curable methacrylate functional groups were then introduced with a urethane reaction between the hydroxyl groups of the microgels and the isocyanate group of isocyanatoethyl methacrylate (IEM). The dual-functional microgels approximately 10 nm in size were compatible with the dual-curable coating formulation. Furthermore, the incorporation of microgels reduced the formulation viscosity. The functional groups in the microgels could participate in UV/thermal curing reactions, and transparent

films were obtained. The effects of the incorporation of microgels on the curing behaviors and mechanical properties of the coatings are discussed.

EXPERIMENTAL

Materials

The chemical structures of the monomers are listed in Table I. Butyl acrylate (BA) and IEM were purchased from Tokyo Chemical Industry Co., Ltd. (Tokyo, Japan). CHA (Bisomer Pemcure 12A) and 1,6-hexanediol diacrylate (HDDA) were supplied from Cognis (Monheim, Germany). Azobisisobutyronitrile (Daejung Chemical Co., Siheung, Korea) was used to initiate polymerization. Dibutyltin dilaurate (DBTDL), 1-dodecanethiol, and methyl ethyl ketone were purchased from Aldrich. Epoxy-acrylate (EA; AgiSyn 1010) was supplied by the AGI Corp (Taipei, Taiwan). A mixture of oxyphenyl acetic acid 2-(2-oxo-2-phenyl acetoxyethoxy)-ethyl ester and oxyphenyl acetic acid 2-(2-hydroxyethoxy)-ethyl ester (Irgacure 754, Ciba, Basel, Switzerland) was used as a photoinitiator. 3,5-Dimethylpyrazole (DMP)-blocked isocyanate based on a hexamethylene diisocyanate trimer (Desmodur PL350, Bayer, Brunsbuttel, Germany) was used as the thermal curing agent. All of the products were used without further purification.

Polymeric microgel synthesis and characterization

HFM was prepared by the copolymerization of CHA, BA, and HDDA with a CHA/BA/HDDA monomer feed molar ratio of 60/35/5 (Fig. 1).

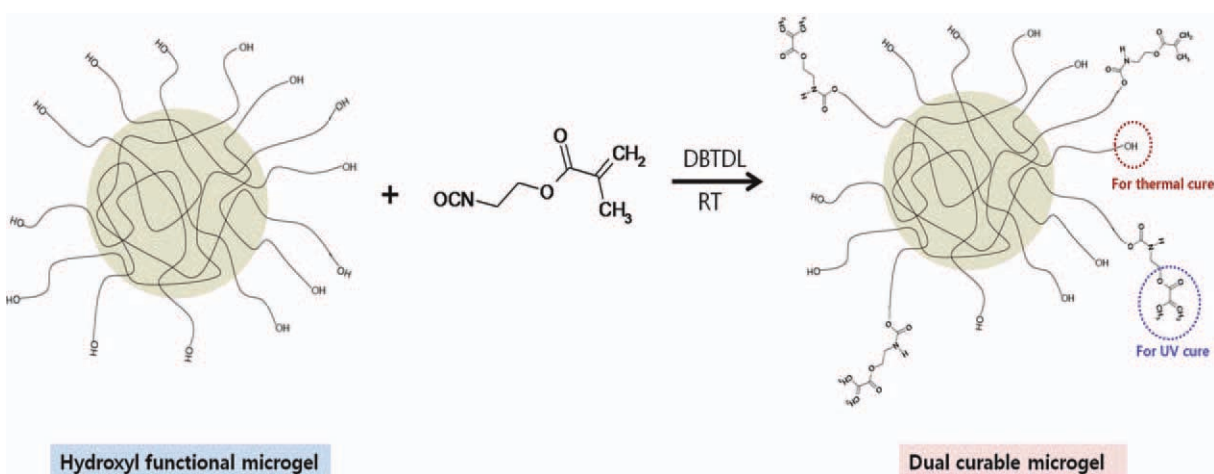


Figure 1 Synthesis of the dual-function microgel by the urethane reaction (RT = room temperature). [Color figure can be viewed in the online issue, which is available at wileyonlinelibrary.com.]

Methyl ethyl ketone was used as the solvent (monomer/solvent = 25/75 wt %). The solvent, the chain-transfer agent (1-dodecanthiol, 2 wt % of total monomer), and 30 wt % of the monomers were put in a reaction vessel fitted with a mechanical stirrer and a reflex condenser and heated to 70°C. The remaining monomers and initiator were added dropwise over 1.5 h. The reaction was stopped after 6 h to achieve a conversion of acrylate double bonds of greater than 95%.¹⁴ The concentration of the initiator was set to 0.65 wt % of the total monomer weight. Next, 10 mol % (HFM10), 30 mol % (HFM30), and 50 mol % (HFM50) of IEM and 0.1 wt % DBTDL were added and stirred overnight at room temperature to ensure the complete reaction between the hydroxyl-functional groups of the microgel and the IEM. The reaction products were analyzed by Fourier transform infrared (FTIR) spectroscopy to confirm that the reaction was complete. Transmission electron microscopy (TEM) analysis was used to characterize the synthesized microgel. A diluted acrylate microgel dispersion (HFM50) was placed onto carbon-coated copper grids, and the copper grids were then exposed to osmium tetroxide vapors for 1 h before TEM observation. The particle size distribution of the synthesized microgel was determined with dynamic light scattering (Malvern Zetasizer Nano-ZS, Malvern, UK).

Characterization of the rheological properties

The rheological properties of the coating solutions were measured with a Haake Mars rheometer (Thermo Scientific, Kalsruhe, Germany). We measured the viscosity of the solutions by increasing the shear rate from 0.001 to 50 1/s. Table II shows the composition of the solution used for the viscosity measurement. The solvent in the microgel dispersions was evaporated in a vacuum oven, and the dried microgels were used for the viscosity measurement.

Formulations and film formation

Table III shows the composition of the coating formulation used to assess the curing behavior and cured coating properties. DMP-blocked isocyanate was used as a thermal curing agent with an NCO/OH molar ratio of 1/1. The photoinitiator concentration was set at 2% of the total weight, and DBTDL was used as a catalyst of the urethane reaction (0.1% of the total weight). The coatings were prepared on a dried waterborne black base coat (supplied by PPG Korea Co., Cheonan, Korea) by spraying, cured by exposure to UV radiation (UV dose = 1200 mJ/cm²), and then cured further at 150°C for 20 min.

TABLE II
Compositions of the Solutions Used for the Viscosity Measurement

Sample ID	0HFM	10HFM	20HFM	30HFM	40HFM	40HFM10	40HFM30	40HFM50
EA	80	70	60	50	40	40	40	40
BA	20	20	20	20	20	20	20	20
HFM		10	20	30	40			
HFM10						40		
HFM30							40	
HFM50								40

TABLE III
Compositions of the Coating Solutions for Analysis of the Curing Behavior and Coating Properties

Sample ID	EA-II	EA-4HFM	EA-12HFM	EA-20HFM	EA-20HFM10	EA-20HFM30	EA-20HFM50	
EA	40	36	28	20	20	20	20	
BA	40	40	40	40	40	40	40	
HFM		4	12	20				
HFM10					20			
HFM30						20		
HFM50							20	
Photoinitiator								2 wt %
DMP-blocked isocyanate								NCO/OH molar ratio = 1/1
DBTDL								0.1 wt %

Characterization of the curing behaviors and coating properties

A rigid-body, pendulum-type testing machine (RPT-3000W, A&D Co., Tokyo, Japan) was used to study the UV and thermal curing behaviors and the physical properties of the cured coatings. Figure 2 shows two types of pendulums: a knife edge type of pendulum for testing the curing behavior and a cylindrical edge type of pendulum for assessing the physical properties [glass-transition temperature (T_g)] of the cured coating samples. The samples were fixed on the cooling and heating blocks, and the pendulum was set such that the fulcrum of the swing contacted the samples vertically. By analyzing the vibration, we obtained the time period of the pendulum swings and the logarithm damping ratio to assess the curing process and the viscoelastic properties.^{15,16} To identify the effects of the microgels on the curing behavior, coating solutions containing microgels were coated on a steel substrate. The temperature was increased from 25 to 150°C for 10 min and maintained for 20 min to assess the thermal curing behaviors with varied amounts of HFM. The UV curing processes were measured with 20 s of UV radiation at 25°C with solutions containing different microgels (HFM10, HFM30, and HFM50).

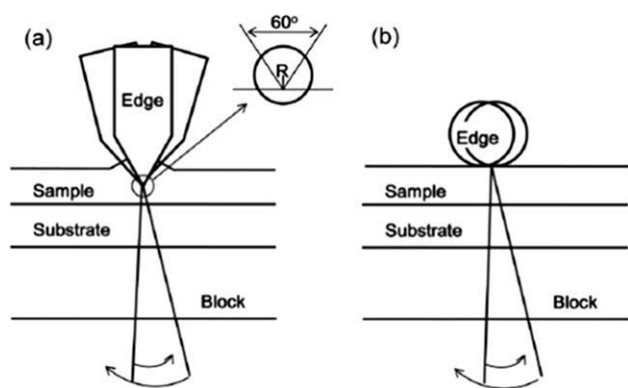


Figure 2 Rigid-body pendulum in the RPT instrument; (a) knife edge type pendulum for testing the curing process, (b) cylindrical edge type pendulum for assessing the physical properties.

The T_g of the dual-cured coatings were also analyzed by RPT. The RPT oven was programmed to heat from 25 to 120°C at a rate of 10°C/min. Scratch tests were carried out on a CSM nanoscratch tester (Peseux, Switzerland) with a spheroconical scratch indenter with a radius of 2 μm and a progressively increased load from 10 to 60 mN for a scratch length of 1 mm at a scanning speed of 2 mm/min. The determination of the critical loads for a coating-substrate system was performed with optical methods. Three scratches were made in different zones for each specimen, and the average values of the load at which the scratch track appeared [first critical load (Lc1)] was determined for each analysis.

RESULTS AND DISCUSSION

Polymeric microgel synthesis and characterization

Figure 3 shows the FTIR spectra of the synthesized microgels. The FTIR analysis was conducted to confirm the reaction between the hydroxyl-functional groups of the HFM and IEM. A peak was not observed in the region of 2250–2270 cm^{-1} belonging to NCO; this indicated that the isocyanate had

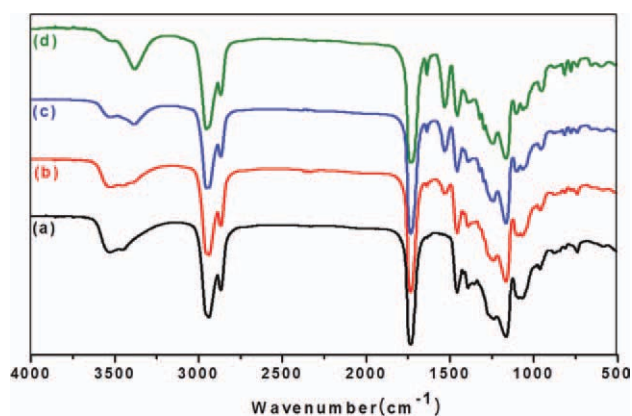


Figure 3 FTIR spectra of the synthesized microgels; (a) HFM, (b) HFM10, (c) HFM30, (d) HFM50. [Color figure can be viewed in the online issue, which is available at [wileyonlinelibrary.com](http://www.interscience.wiley.com).]

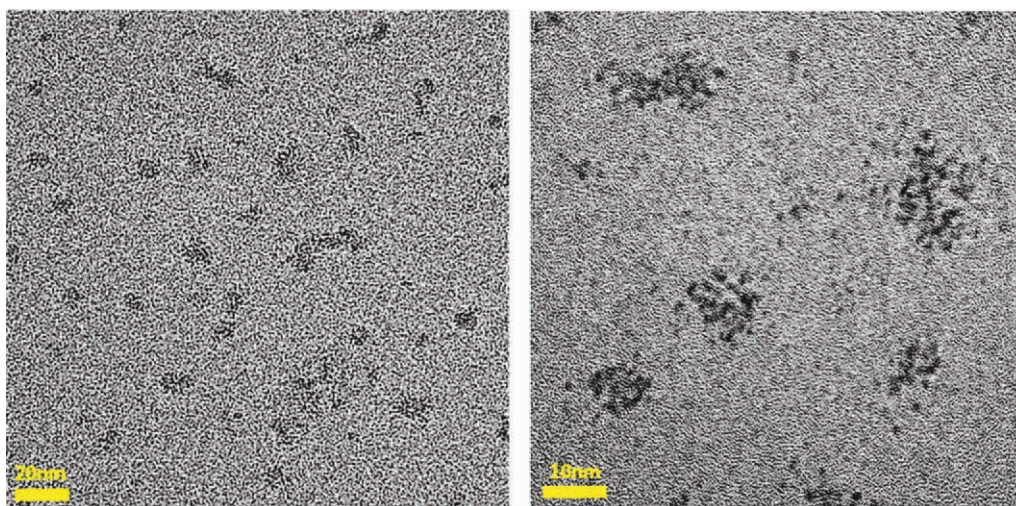


Figure 4 TEM micrograph of acrylate microgel (HFM50) stained with OsO_4 vapors. [Color figure can be viewed in the online issue, which is available at wileyonlinelibrary.com.]

reacted completely. In addition, with greater IEM contents, the peak intensities at 1530 cm^{-1} (N—H) and $3330\text{--}3360\text{ cm}^{-1}$ (N—H) increased, and the OH peak intensity at 3500 cm^{-1} decreased. This observation indicated that a urethane linkage formed through the reaction between the IEM and OH groups of the microgel. The number of degree of hydrogen bonding could be obtained by the determination of the magnitude of N—H and C=O stretching of the urethane or urea groups.¹⁷ As the amount of IEM in the microgel increased, the N—H peak gradually shifted to lower wave numbers. These results confirmed that the hydrogen bonding of microgels increased with IEM content. The acrylate peak ($\sim 1630\text{ cm}^{-1}$) also increased because of the acrylate functional groups of the IEM.¹⁸ FTIR analysis showed that dual-curable microgels containing both OH and methacrylate were successfully synthesized. Figure 4 shows TEM images of the HFM50 microgel stained with OsO_4 vapors. TEM was used to observe the microgel particle size. Their average dry particle size was approximately 10 nm. The microgel particles did not show a regular morphology, such as a spherical shape, but a deformed aggregated morphology because of the low T_g of microgels containing linear flexible stabilizer chains. Regardless, the particle size of the microgels was much smaller than the visible light wavelength, such that the synthesized microgels could be incorporated into a clear coating formulation without any harmful effects on the coating transparency.

Figure 5 shows the particle size distribution of HFM50. The measured z-average hydrodynamic diameter of HFM50 was 9.9 nm. This result also showed that the nanosized microgel was successfully synthesized.

Effects of the microgels on the rheological properties

To evaluate the effects of the microgels on the rheological properties of the solutions, viscosity measurements were conducted with microgel-containing solutions. Figure 6(a) shows the results of the viscosity measurements of solutions containing different amounts of HFM. The results show that the incorporation of microgels significantly reduced the solution viscosity, and a greater reduction in the viscosity was obtained with increasing microgel content. Because of their internal crosslinking, the synthesized microgels had a very compact structure, and the particles could not overlap each other.^{19,20} Only the short segments located at the microgel surface could interact, so the chain entanglement was greatly reduced. Consequently, the viscosity of the solutions was reduced with the addition of the

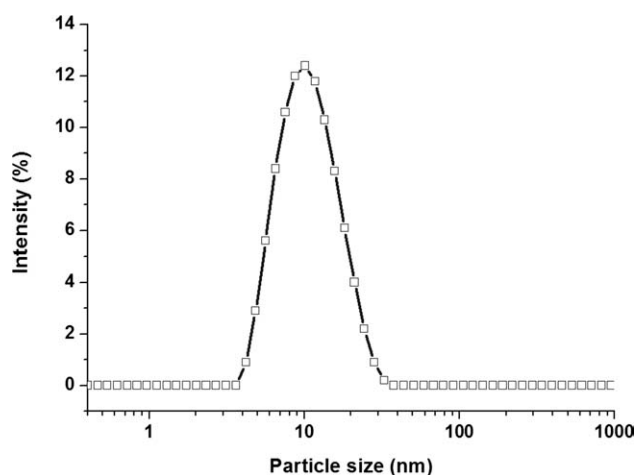


Figure 5 Particle size distribution of HFM50.

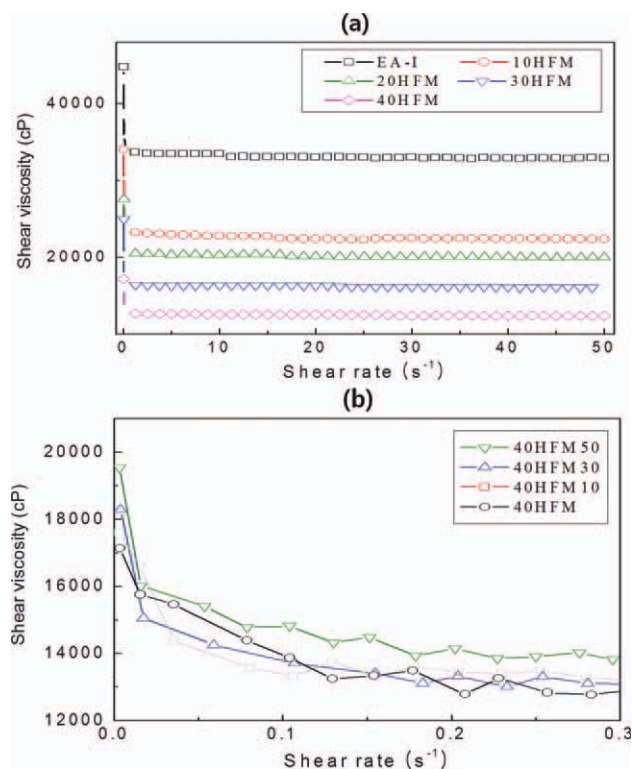


Figure 6 Rheological properties of the coating solutions containing (a) different contents of HFM and (b) different microgels (HFM, HFM10, HFM30, and HFM50). [Color figure can be viewed in the online issue, which is available at wileyonlinelibrary.com.]

microgels. Thus, it was possible to decrease the amount of volatile organic compounds in the coating formulation through application of the synthesized microgel. Figure 6(b) shows the results of the viscosity measurements of solutions containing different microgels at a very low shear rate. Microgels containing a greater IEM content showed a greater extent of shear thinning behavior at a low shear rate because of the hydrogen bonding of the urethane linkage. Shear thinning behavior is especially interesting for paint in spray applications, in which a low viscosity is required during application under a high shear rate and a high viscosity is needed under a low shear rate to reduce sagging problems. Thus, the higher viscosity at a lower shear rate in this microgel-containing formulation was helpful for minimizing sagging problems.

Effects of the microgels on the curing behavior

The UV curing behaviors of solutions containing different microgels are shown in Figure 7. After UV irradiation, the oscillation period decreased rapidly and became flatter; this indicated that the curing reaction had reached a balanced state. The UV curing process was too rapid to compare the effects of the microgel on the curing speed. However, a lower

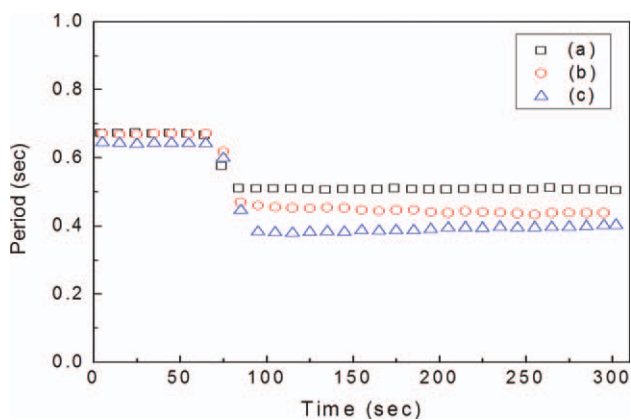


Figure 7 UV curing behaviors of coating solutions containing (a) EA-20HFM10, (b) EA-20HFM30 and (c) EA-20HFM50. [Color figure can be viewed in the online issue, which is available at wileyonlinelibrary.com.]

equilibrium oscillation period was obtained because of the increased number of acrylate functional groups of the microgel. Thus, the acrylate functional groups of the microgel participated in the UV curing process, and the crosslink density was higher with higher acrylate contents. Figure 8 shows the thermal curing behaviors of the coating solutions. During the curing period, the oscillation period decreased gradually because the viscosity of the test sample increased. In addition, the slope of the curing curve provided information on the curing speed of the coating solution.²¹ The results show that the onset of the crosslinking reaction occurred at an earlier time with a faster curing speed with increasing HFM content; this effect occurred because the microgel had a greater number of reactive primary hydroxyl groups compared to secondary groups of the EA oligomer. FTIR analysis was used to examine the chemical functionality of the cured films. The spectra of the UV/thermal dual-cured films are shown in Figure 9.

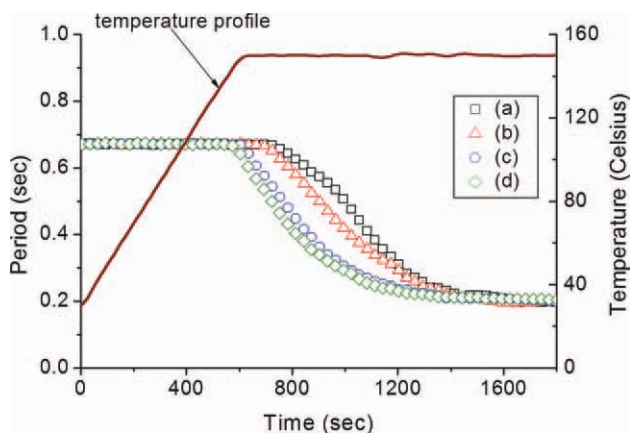


Figure 8 Thermal curing behaviors of (a) EA-II, (b) EA-4HFM, (c) EA-12HFM and (d) EA-20HFM. [Color figure can be viewed in the online issue, which is available at wileyonlinelibrary.com.]

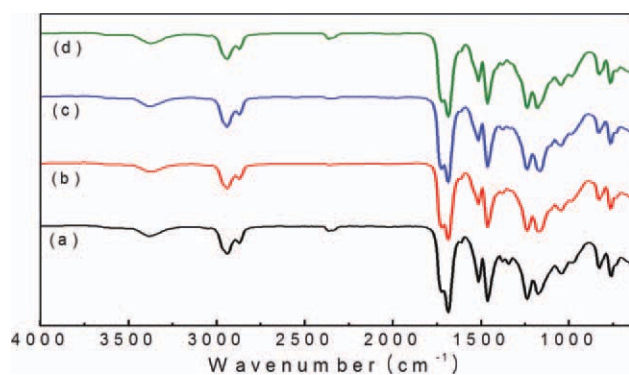


Figure 9 FTIR spectra of dual cured films (a) EA-II, (b) EA-20HFM10, (c) EA-20HFM30, and (d) EA-20HFM50. [Color figure can be viewed in the online issue, which is available at wileyonlinelibrary.com.]

A peak belonging to NCO in the region 2250–2270 cm^{-1} was observed for all specimens; this peak came from a deblocking reaction of the blocked isocyanate crosslinker (Desmodur PL-350). A stronger absorption of NCO was found for the dual-cured epoxy-acrylate film (EA-II) and EA-20HFM50 relative to the other films containing the microgels, and the peak intensity increased with increasing acrylate functionality of the microgel. This result indicates that some of the unblocked isocyanates remained unreacted after the thermal curing process. In the case of EA-II, a greater number of isocyanate groups were not reacted with hydroxyl groups because of the lower abundance of primary hydroxyl groups and low reactivity of the secondary hydroxyl in the EA. On the other hand, in the case of EA-20HFM50, a greater extent of crosslinking occurred in the UV curing process with increasing acrylate functional groups of the microgel; this hindered the formation of urethane linkages during thermal curing. This meant that there was some degree of vitrification of the film after the UV curing of the EA-20HFM50 system, and this strongly limited the completion of the crosslinking reaction.

Effects of the microgel on the physical properties of the coatings

The logarithmic damping ratios of the dual-cured-coating-containing microgels are shown in Figure 10. The values of T_g depended on the chemical structure. The flexibility of the molecular chain depended on free-volume theory, and thermodynamic theory was one of the factors influencing the value of T_g . EA-II appeared to have a T_g at 97°C due to the presence of the rigid aromatic backbone of EA. In comparison, the cured-film-containing microgels had a lower T_g of approximately 60–70°C. Although the microgels were reactive with the matrix polymer and increased the overall crosslinking density, T_g decreased with the addition of microgels. The incor-

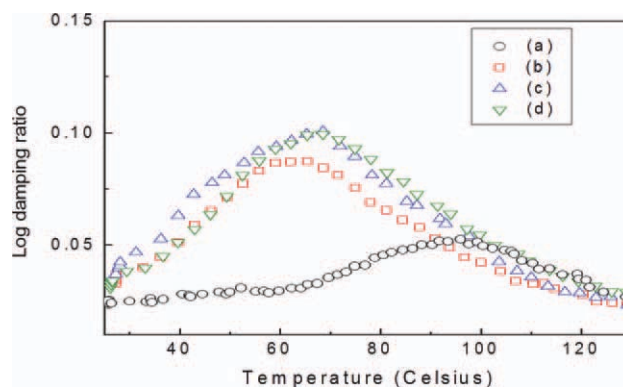


Figure 10 T_g of the dual-cured films (a) EA-II, (b) EA-20HFM10, (c) EA-20HFM30 and (d) EA-20HFM50. [Color figure can be viewed in the online issue, which is available at wileyonlinelibrary.com.]

poration of microgels in the coating formulation lowered the T_g of the cured film because of the flexible stabilizer chains containing functional groups. The nanoscratch properties of each cured sample were measured to investigate the effect of the microgels on the scratch resistance. Figure 11 shows optical images of the damage after the scratch tests and the Lc1 values at which the scratch track appeared for the different coating films. The results show that the coating-containing microgels had a greater resistance to scratching. Deformation is understood to consist of three components: elastic, ductile, and brittle.²² Ductile deformation is made of an elastic component, which can recover with time, and a plastic component, which is not recoverable. Brittle deformation introduced cracks at a certain critical load. The addition of microgels to the brittle EA-based coating increased the flexibility and toughness of the matrix because the microgel had internal crosslinking and chemical bonding with the matrix by a curable flexible stabilizer. The increased ductility and toughness with soft microgel incorporation increased the scratch resistance of the EA-based coating.²³

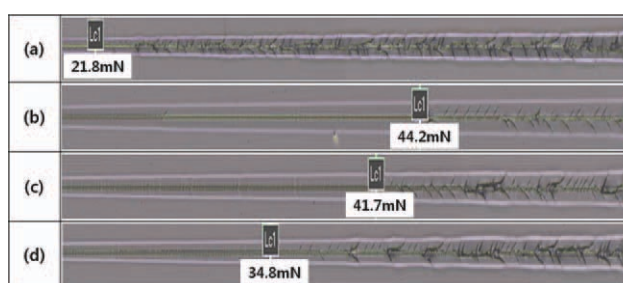


Figure 11 Optical images of damage after the scratch tests and Lc1 at which the scratch track appeared for the different coatings (a) EA-II, (b) EA-20HFM10, (c) EA-20HFM30 and (d) EA-20HFM50. [Color figure can be viewed in the online issue, which is available at wileyonlinelibrary.com.]

CONCLUSIONS

Nanosized dual-function (hydroxyl and methacrylate) microgels were synthesized with CHA as a stabilizer and IEM as a methacrylate functional monomer. On the basis of the FTIR spectra, TEM analysis, and dynamic light scattering measurements, we concluded that dual-functional microgels about 10 nm in size were successfully synthesized. The synthesized microgels were compatible with the dual-curable coating solution based on an EA oligomer and could be successfully used in a clear coat formulation without any detrimental effects on the coating transparency. The application of the microgels in the coating formulations was beneficial for reducing the VOC content because of the reduction in the viscosity and was useful for inhibiting sagging problems because of shear thinning behavior. Because the functional groups in the microgels participated in the UV and thermal crosslinking reactions, the addition of the microgel affected the mechanical properties of the matrix. T_g of the cured films decreased with the addition of the microgel because of the flexible functional stabilizer chains. The increased ductility and toughness of the coating with the addition of flexible microgels increased the scratch resistance of the EA oligomer-based dual-cure coating.

References

1. Tey, J. N.; Soutar, A. M.; Priyadarshi, A.; Mhaisalkar, S. G.; Hew, K. M. *J Appl Polym Sci* 2007, 103, 1985.
2. Deflorian, F.; Fedel, M.; Digianni, A.; Bongiovanni, R.; Turri, S. *Corros Eng Sci Tech* 2008, 43, 81.
3. Shi, W.; Ranby, B. *J Appl Polym Sci* 1994, 51, 1129.
4. Studer, K.; Decker, C.; Beck, E.; Schwalm, R. *Eur Polym J* 2005, 41, 157.
5. Chang, C.-W.; Lu, K.-T. *J Appl Polym Sci* 2010, 115, 2197.
6. Turner, J. L.; Wooley, K. L. *Nano Lett* 2004, 4, 683.
7. Nguyen, L. H.; Straub, M.; Gu, M. *Adv Funct Mater* 2005, 15, 209.
8. Zhang, G.; Niu, A.; Peng, S.; Jiang, M.; Tu, Y.; Li, M.; Wu, C. *Acc Chem Res* 2001, 34, 249.
9. Valette, L.; Pascault, J.-P.; Magny, B. *Macromol Mater Eng* 2003, 288, 867.
10. Valette, L.; Pascault, J.-P.; Magny, B. *Macromol Mater Eng* 2003, 288, 642.
11. Sa, S.; Zhang, B.; Yang, Q.; Wang, X.; Mao, Z. *J Shanghai Univ* 2009, 13, 67.
12. Kim, Y.-B.; Kim, H.-K.; Hong, J.-W. *Surf Coat Technol* 2002, 153, 284.
13. Rouzeau, S.; Mechin, F.; Pascault, J. P.; Magny, B. *Eur Polym J* 2002, 43, 4398.
14. Valette, L.; Pascault, J. P.; Magny, B. *Macromol Mater Eng* 2002, 287, 31.
15. Lee, B. H.; Choi, J. H.; Kim, H.-J.; Kim, J. I.; Park, J. Y. *J Ind Eng Chem* 2004, 10, 608.
16. Chiu, H.-T.; Cheng, J.-O. *J Appl Polym Sci* 2008, 108, 3973.
17. Yilgor, E.; Yurtserver, E.; Yilgor, I. *Polymer* 2002, 43, 6561.
18. Studer, K.; Decker, C.; Beck, E.; Schwalm, R.; Gruber, N. *Prog Org Coat* 2005, 53, 126.
19. Pakula, T.; Geyler, S.; Edling, T.; Boese, D. *Rheol Acta* 1996, 35, 631.
20. Pakula, T. *Recent Res Dev Polym Sci* 1996, 1, 101.
21. Chiu, H.-T.; Cheng, M.-F. *J Appl Polym Sci* 2006, 101, 3402.
22. Chapiro, A. *Radiation Chemistry of Polymer Systems*; Wiley/Interscience: New York, 1962; p 1979.
23. Sangermano, M.; Messori, M.; Galleco, M. M.; Rizza, G.; Voit, B. *Polymer* 2009, 50, 5647.